The Journal of Clinical Endocrinology & Metabolism, 2021, Vol. 106, No. 5, e2271–e2289
doi:10.1210/clinem/dgab027
Clinical Research Article

Clinical Research Article

Investigation of Mechanical, Material, and Compositional Determinants of Human Trabecular Bone Quality in Type 2 Diabetes

Praveer Sihota,[1,*] Ram Naresh Yadav,[1,*] Ruban Dhaliwal,[2] Jagadeesh Chandra Bose,[3] Vandana Dhiman,[4] Deepak Neradi,[5] Shailesh Karn,[5] Sidhartha Sharma,[5] Sameer Aggarwal,[5] Vijay G. Goni,[5] Vishwajeet Mehandia,[1] Deepak Vashishth,[6] Sanjay Kumar Bhadada,[4] and Navin Kumar[1]

[1]Department of Mechanical Engineering, Indian Institute of Technology Ropar, Rupnagar, Punjab, 140001, India; [2]Metabolic Bone Disease Center, State University of New York, Upstate Medical University, Syracuse, NY 13210, USA; [3]Department of Internal Medicine, Post Graduate Institute of Medical Education and Research, Chandigarh, 160012, India; [4]Department of Endocrinology, Post Graduate Institute of Medical Education and Research, Chandigarh, 160012, India; [5]Department of Orthopedics, Post Graduate Institute of Medical Education and Research, Chandigarh, 160012, India; and [6]Department of Biomedical Engineering, Center for Biotechnology and Interdisciplinary Studies, Rensselaer Polytechnic Institute, Troy, NY 12180, USA

ORCiD numbers: 0000-0003-4179-4006 (R. Dhaliwal); 0000-0002-0410-8778 (S. K. Bhadada); 0000-0002-7958-8155 (N. Kumar).

*These authors contributed equally.

Abbreviations: μ-CT, microcomputed tomography; aBMD, areal bone mineral density; AGE, advanced glycation end-product; ANCOVA, analysis of covariance; BV/TV, bone volume fraction; DA, degree of anisotropy; E-xLR, enzymatic crosslink ratio; fAGE, fluorescent advanced glycation end-product; FTIR, Fourier transform infrared spectroscopy; HbA1c, glycosylated hemoglobin A1c; NE-xLR, nonenzymatic crosslink ratio; SMI, structure model index; T2D, type 2 diabetes; Tb.Sp, trabecular separation; Tb.Th, trabecular thickness; TGA, thermogravimetric analysis; XRD, X-ray diffraction.

Received: 21 July 2020; Editorial Decision: 12 January 2021; First Published Online: 21 January 2021; Corrected and Typeset: 16 February 2021.

Abstract

Context: Increased bone fragility and reduced energy absorption to fracture associated with type 2 diabetes (T2D) cannot be explained by bone mineral density alone. This study, for the first time, reports on alterations in bone tissue's material properties obtained from individuals with diabetes and known fragility fracture status.

Objective: To investigate the role of T2D in altering biomechanical, microstructural, and compositional properties of bone in individuals with fragility fracture.

Methods: Femoral head bone tissue specimens were collected from patients who underwent replacement surgery for fragility hip fracture. Trabecular bone quality parameters were compared in samples of 2 groups, nondiabetic (n = 40) and diabetic (n = 30), with a mean duration of disease 7.5 ± 2.8 years.

ISSN Print 0021-972X ISSN Online 1945-7197
Printed in USA

Results: No significant difference was observed in aBMD between the groups. Bone volume fraction (BV/TV) was lower in the diabetic group due to fewer and thinner trabeculae. The apparent-level toughness and postyield energy were lower in those with diabetes. Tissue-level (nanoindentation) modulus and hardness were lower in this group. Compositional differences in the diabetic group included lower mineral:matrix, wider mineral crystals, and bone collagen modifications—higher total fluorescent advanced glycation end-products (fAGEs), higher nonenzymatic cross-link ratio (NE-xLR), and altered secondary structure (amide bands). There was a strong inverse correlation between NE-xLR and postyield strain, fAGEs and postyield energy, and fAGEs and toughness.

Conclusion: The current study is novel in examining bone tissue in T2D following first hip fragility fracture. Our findings provide evidence of hyperglycemia's detrimental effects on trabecular bone quality at multiple scales leading to lower energy absorption and toughness indicative of increased propensity to bone fragility.

Key Words: diabetes, bone quality, AGEs, trabecular bone, fragility fracture, bone toughness

Type 2 diabetes (T2D) affects bone homeostasis leading up to 3-fold increased hip fracture risk compared with those without diabetes (1-3). This high fragility fracture risk is observed despite adequate areal bone mineral density (aBMD) in T2D (4-9). Thus, aBMD underestimates fracture risk in T2D, making the clinical identification of those at risk for fractures difficult. Beyond aBMD, the key factors contributing to bone strength are the parameters of bone quality—microstructure, bone material properties, bone mineral content and mean crystal size, bone protein (Amide I and II) quantity and its secondary structure, and bone cell activity and dynamics (Fig. 1A). These determinants have been examined individually in few studies and material properties are often listed as the cause of poor bone quality in diabetes (10-13). Only animal studies (14-19) and 3 recent studies of human tissue have attempted to address this question comprehensively (10, 11, 13). A limitation of the previous human studies is that bone tissue was collected at the time of arthroplasty and may therefore have confounding effects associated with arthritis (including increased trabecular bone density) (10, 11, 13). Furthermore, no prior studies of bone tissue material properties in humans have been conducted with known diabetic status and known fragility fracture status. The current study is novel in examining human bone tissue following first hip fragility fracture.

The mechanisms underlying this poor bone quality and high fracture risk in diabetes are not well understood. Prolonged hyperglycemia leads to an increase in the nonenzymatic reactions (Maillard reactions) and the formation of advanced glycation end-products (AGEs) through post-translation modification (20). AGEs then accumulate in the bone tissue and react irreversibly with amino acid residues of peptides or proteins to form protein adducts or protein crosslinks (21). This phenomenon, widely recognized as nonenzymatic crosslinking (NE-xL), is the underlying mechanism for multiple complications of diabetes, as it alters normal cellular functioning and tissue quality (22, 23). AGE accumulation may also alter mineralization through hyperglycemia affecting bone strength (15).

In the present ex vivo study, we aimed for multiscale characterization of bone tissue from individuals with and without diabetes, following hip fracture. This study includes investigation of the structural parameters at voxel size consistent with use of microcomputed tomography (μ-CT) and corresponding apparent level mechanical properties measured through the uniaxial compression test. We also examine bone material properties (nanoindentation) as well as bone composition (thermogravimetric analysis [TGA]), mineral crystal size (X-ray diffraction [XRD]), alterations in protein content, enzymatic crosslink ratio (E-xLR), nonenzymatic crosslink ratio (NE-xLR) (Fourier transform infrared spectroscopy [FTIR]), and fluorescent (f)AGE content in the human diabetic bone tissue.

Material and Methods

Study Participants

Bone samples were taken from 2 groups of patients who underwent bipolar hemiarthroplasty or total hip replacement following fragility fracture of hip—patients without diabetes (n = 40) and with diabetes (n = 30). Replacement surgery was the recommended treatment as these hip fractures were unsuitable for management with cannulated cancellous screw or proximal femoral nail. Patients' age also favored replacement surgery for better outcome. T2D was diagnosed according to the American Diabetes Association criteria (24). None of the patients had history of hip fracture prior to the fracture reported

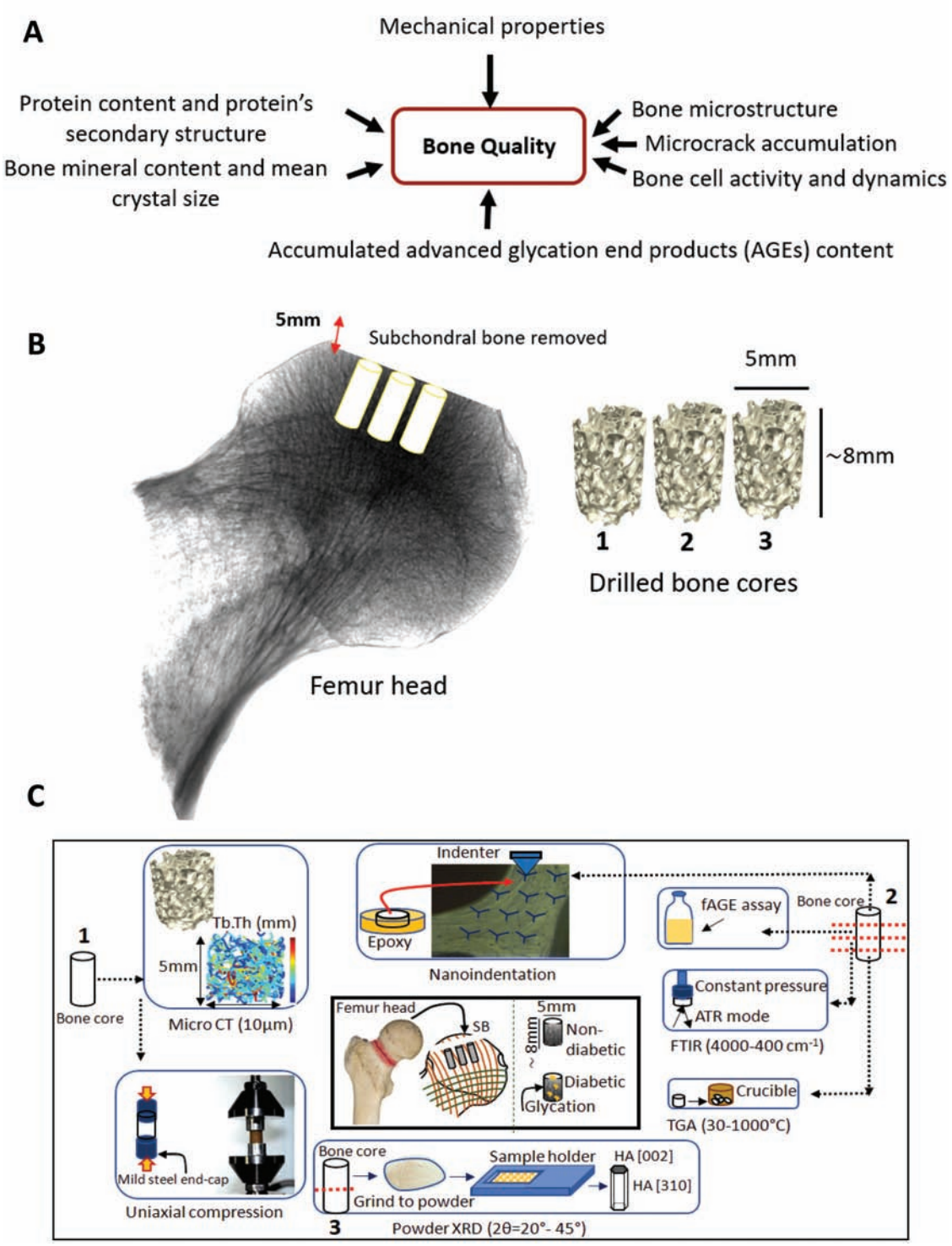

Figure 1. (A) Determinants of bone quality, (B) The extraction of cylindrical trabecular bone cores, each 5 mm in diameter and 8-9 mm in length, from femoral heads along the direction of the principal trabeculae using the drilling machine attached with diamond core bit, (C) Characterization techniques used to determine the human trabecular bone quality for diabetes patients. SB, subchondral bone.

here. Patients with cancer, osteoarthritis, renal dysfunction, primary or secondary hyperparathyroidism, unexplained elevated alkaline phosphatase, and secondary osteoporosis (chronic steroid or antiepileptic use) were excluded from the study.

All patients with diabetes were taking antidiabetic medications (metformin, sulfonylurea, or insulin). None were on pioglitazone or SGLT2 inhibitors. All participants involved in the study were from Northern India. The study was approved by the Institutional Ethics Committee (Approval

Number PGI/IEC/2015/171) of the Postgraduate Institute of Medical Education and Research, Chandigarh. Written informed consent was obtained from each study participant. Demographic, clinical, biochemical, and aBMD (contralateral femoral neck BMD) were recorded for all participants.

Sample Procurement and Storage

Femoral heads were collected from patients undergoing replacement surgery for hip fractures. From each femoral head, 5 to 7 cylindrical trabecular bone cores, each 5 mm in diameter and 8 to 9 mm in length, were extracted from femoral heads along the direction of the principal trabeculae using the drilling machine attached with a diamond core bit as shown in (Fig. 1B). The bone cores were cleaned with a water jet, wrapped in saline-soaked gauze (PBS 7.4 pH), transferred into sample bags, labeled, and subsequently stored at –20°C (10). Bone cores were then used for different characterization techniques, as shown in (Fig. 1C). All experiments were conducted within 1 month after the collection of the femoral head.

Assessment of Bone Quality Parameters

Microstructural parameters

The microstructural parameters were studied using μ-CT. One bone core of each patient was air dried and scanned along the cylindrical axis on a μ-CT system (Phoenix/x-ray, GE Sensing & Inspection Technologies, Germany) using 10 μm voxel size, 45 keV tube voltage, 250 μA beam current, 250 second integration time, and 10 frames. Reconstruction of scanned images was collected using Phoenix software (phoenix/x-ray, GE Measurement & Control; Germany) and reconstructed images were imported in Scan-IP (Simpleware Ltd, UK) and Image J's plugin BoneJ (software by National Institute of Health, https://imagej.nih.gov/ij/) (25). Following structural parameters were obtained: bone volume fraction (BV/TV), trabecular thickness (Tb.Th), trabecular separation (Tb.Sp), trabecular number (Tb.N), structure model index (SMI), and degree of anisotropy (DA) (26).

Bulk mechanical properties

After μ-CT imaging, the bone cores were utilized for compression testing. The samples were rehydrated in saline-soaked gauzes for 2 hours at 4°C. Mean specimen length of 8 mm and length to diameter ratio of nearly 1.5:1 were used for testing. The bone cores were glued in customized mild steel cylindrical end caps to minimize end-effects (27). A compression test was performed on each core to measure the mechanical properties using an electromagnetic testing system (Electroforce 3200, Bose, Eden Prairie, MN, USA, with specification of load cell: ±450 N, and linear variable displacement transducer: stroke length ±6.5 mm with 0.1 μm resolution) at room temperature while keeping the specimen hydrated in phosphate-buffered saline spray (28). The specimens were preloaded to 5 N to ensure proper contact between the test specimen and the compression plate. Then, preconditioning between 0.05% and 0.2 % strain was done in 3 cycles to minimize the toe region. Montontic testing was conducted at a strain rate of 0.01 s^{-1} until 1 mm displacement. The load displacement data were captured at 100 Hz frequency and converted into stress–strain data (Fig. 2A), to determine several mechanical parameters including elastic modulus, yield point (using the 0.2% offset method), ultimate point (determined as the point of maximum load), postyield strain (determined as the difference between ultimate strain and yield strain), postyield strain energy, and toughness (27, 29, 30).

Bone material properties

The bone material properties were determined using nanoindentation. A bone core from each patient was embedded in epoxy and used to determine material level properties via nanoindentation. The embedded samples were ground, polished in diamond solutions with particle sizes of 3, 1, 0.25, and 0.05 μm (Buehler Eco Met 250 grinder

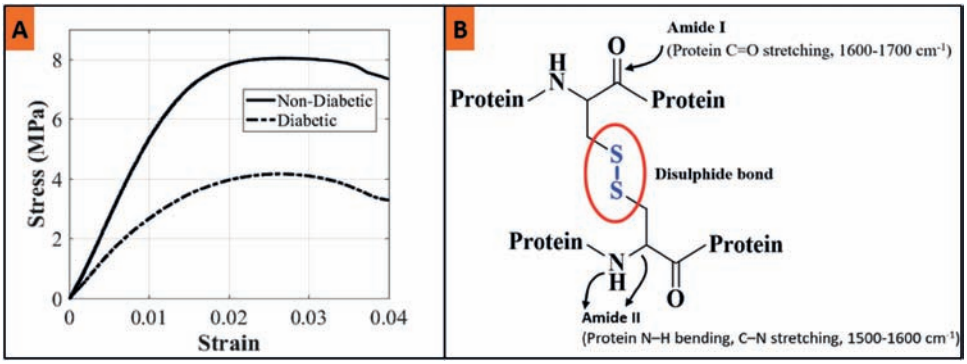

Figure 2. (A) Calculated typical stress–strain plot of compression test for diabetic and nondiabetic groups, (B) Amide I and Amide II bond positions in principal structural unit of collagen in human trabecular bone.

and polisher) and abrasive papers of 1200, 2000, and 4000 grit sizes, under the water cooling condition. The samples were cleaned ultrasonically with distilled water between each polishing step.

Nanoindentation tests were performed using a TI-950 Tribo Indenter (Hysitron Inc., Minneapolis, MN, USA) with Berkovich pyramidal tip, having an included angle of 142.3° and tip radius of ~150 nm. The calibration of the instrument was performed using standard fused quartz and aluminum samples following the standard procedure (31, 32). Locations for indents were identified using an in situ scanning probe microscope integrated with the nanoindentation system. All tests were performed at room temperature in moist conditions.

Twenty (20) indents with a peak load of 3000 μN were applied to the longitudinal sections of the core (33). The load function consisted of a 10-second ramp to peak force segment, followed by a 30-second hold and an unloading segment of 10 second. The 30-second hold time was adopted to eliminate creep effects (34). The load displacement curves, obtained from indentation tests, were analyzed to determine the reduced modulus (Er) and hardness (H) (average of 20 indents) using Oliver and Pharr method in Triboscan (Hysitron) (35, 36).

Composition

TGA was performed to compare the bulk mineral to matrix ratio. Approximately 8 to 12 mg of trabecular bone underwent TGA (TGA/DSC1 instrument, Mettler Toledo, Greifensee, Switzerland) in a controlled air atmosphere from room temperature to 1000°C with a heating rate of 10°C/min. The thermal data were analyzed in STARe software (version 12.1). The mineral to matrix ratio was calculated as the ratio between the percentages of mass (% dry weight) remaining after heating to 600°C and the organic mass loss between 200°C and 600°C. The protocol was adopted from published studies (37, 38).

Mean crystal size

In order to obtain a powder, the half bone core was defatted and dehydrated in increasing concentrations of ethanol (70% to 100%) for 10 minutes each. The specimen was wet ground in acetone using a mortar and pestle until a uniform and homogeneous powder was obtained (31). XRD measurements were performed using CuKα radiation at 40 kV and 40 mA (X'Pert PRO, PANalytical) from 20 to 45° 2θ. The X'pert Highscore plus software was used for background correction and to fit the diffraction peaks at 2θ = 26° and 40° corresponding to 002 (c-axis direction) and 310 planes (ab-plane), respectively. The data of 002 and 310 planes were utilized to calculate the average length and width of mineral crystal respectively using the Scherrer equation (39-41).

Mineral and collagen properties

FTIR spectra were recorded from the freeze-dried bone section of donors using Bruker IFS 66v/S FTIR spectrophotometer in the attenuated total reflectance mode, under constant pressure, in the spectral region of 4000 to 400 cm^{-1} and used to calculate the following parameters: carbonate to phosphate ratio (area ratio of the carbonate ν2 peak [852-890 cm^{-1}] to phosphate ν1-ν3 peak [916–1180 cm^{-1}]), mineral crystallinity [intensity ratio of 1030 cm^{-1} to 1020 cm^{-1}, which is related to crystal size and stoichiometric perfection], and the acid phosphate content (intensity ratio of 1127 cm^{-1} to 1096 cm^{-1}, which characterizes acid phosphate substitution into stoichiometric hydroxyapatite) (42, 43). The Amide I band (Fig. 2B) possesses structural information about the collagen matrix and is also the location of the strongest peaks for the nonenzymatic crosslink pentosidine (22). Thus, sub-bands of the Amide I band were fitted with Gaussian curves at 1610, 1630, 1645, 1660, 1678, and 1692 cm^{-1} by using a peak analyzer tool in OriginPro 8.5 software. These peaks were chosen based on the second derivative approach. From the analysis of Amide I sub-bands, the NE-xLR (22), and E-xLR (44) were measured through the area ratio of the 1678/1692 cm^{-1} and 1660/1678 cm^{-1} sub-bands, respectively. The measurement of NE-xLR enables the estimation of overall AGE content in bone tissue itself (22). Also, the collagen maturity (area ratio of 1660 cm^{-1} to 1690 cm^{-1}) was measured within the Amide I peak (44, 45). The integrated area ratio (relative content) of Amide I and Amide II (46-48) bands were normalized with respect to the methylene (CH_2) deformation band at 1450 cm^{-1}, similar to previous studies (48, 49). Finally, the mineral to matrix ratio (area ratio of the phosphate ν1-ν3 peak [916-1180 cm^{-1}] to amide I peak [1596-1712 cm^{-1}]) was measured (42, 43).

Fluorescent Advanced Glycation End-products assay

Total fAGEs were measured using fluorescence spectrometry and normalized to collagen concentration similar to previous studies (50, 51). The quarter bone cores of each donor were lyophilized overnight then 45 to 55 mg of dried specimens was hydrolyzed in 6 N HCl (100 μL/mg bone) at 110°C for 20 hours in hydrolysis vials with screw caps. The hydrolysates were cooled in room temperature, collected in a microcentrifuge tube, and centrifuged with 13 000 rpm at 4°C (Eppendorf 5424R microcentrifuge). The supernatant was collected, diluted (10 times with DI water), and fluorescence was measured in a flat bottom 96-well plate using a multimode microplate reader (CLARIOstar Plus, BMG LABTECH) at an excitation of 360 nm and an emission of 460 nm. The fluorescence data of specimens were normalized with serially diluted quinine standards (stock: 10 μg quinine per 1 mL of 0.1 N H_2SO_4) measured in the same way (50,

51). Next, the absorbance assay of hydroxyproline was performed to determine collagen content to normalize the total fluorescence (50). Total fAGEs are reported in units of nanograms of quinine fluorescence per milligram of collagen. The collagen content is derived based on prior knowledge that collagen consists of 14% hydroxyproline (52). All solutions used were freshly prepared, and experiments were performed in darkness at room temperature.

Statistical Analysis

Distributions of mechanical properties were plotted to identify potential outliers, and the data from 5 donors (3 from the nondiabetic group and 2 from the diabetic group) with values 2 SD beyond the mean were removed from all analysis. The distribution of the data was tested for normality by the Kolmogorov–Smirnov test. Homogeneity of variances was analyzed using Levene's test. Between-group differences of calculated parameters were analyzed for statistical significance using Student's t-tests, after testing for normality and homogeneity of variances. Mean values and standard deviation were calculated for the measured parameters. Pearson correlation tests were used to determine relationships between variables. Forward stepwise regression tests were conducted for mechanical properties using all significant parameters as independent variables. An analysis of covariance (ANCOVA) was conducted to compare the differences in mechanical properties among groups by using BV/TV as a covariate. Post hoc power calculation was performed by comparing the mean value of postyield energy and toughness between diabetic and nondiabetic groups using an ANOVA test. A confidence level of $P < .05$ implies a statistical significance between the groups where $P < .05$, $P < .01$, and $P < .001$ denote the level of significance. Statistical analysis was performed using SPSS (v.21, SPSS Inc., Chicago, IL, USA) and Microsoft Office Excel (2007).

Results

Patient Characteristics

Table 1 shows the baseline characteristics of patients with diabetes (n = 30) and without diabetes (n = 40). The mean age of the diabetic and nondiabetic group was 69.7 ± 10.0 and 69.8 ± 10.2 years, respectively. The sex distribution among groups was also similar. Other than preoperative glycosylated hemoglobin A1c (HbA1c) levels, no significant differences were observed in other baseline characteristics, including aBMD, T score, and biochemical parameters between diabetic and nondiabetic groups. The duration of diabetes ranges from 4 to 15 (7.5 ± 2.8) years.

Microstructural Parameters

Representative μ-CT images and map of trabecular thickness in diabetic and nondiabetic bones are shown in (Fig. 3),

Table 1. Baseline demographic, radiographic and biochemical parameters of diabetic and nondiabetic groups

Parameters	Nondiabetic group (n = 40)	Diabetic group (n = 30)	*P* value
Gender (females) n, %	25, 62.5	19, 63.3	.198
Age (years)	69.8 ± 10.2	69.7 ± 10.0	.961
Biochemical			
Preoperative HbA1c (%)	5.4 ± 0.4	7.9 ± 1.8	<.001
Diabetes duration (years)	na	7.5 ± 2.8	na
Serum calcium (mg/dL)	8.4 ± 0.6	8.5 ± 0.6	.306
Serum phosphorus (mg/dL)	3.4 ± 0.7	3.4 ± 0.6	.658
PTH (pg/mL)	39.3 ± 21.0	41.4 ± 38.4	.791
25-hydroxy Vitamin D (ng/mL)	22.3 ± 8.6	22.5 ± 8.5	.932
ALP (IU/L)	134.2 ± 75.8	131.2 ± 36.9	.875
Imaging			
FN aBMD (gm/cm^2)	0.600 ± 0.091	0.578 ± 0.106	.329
FN T score	–2.6 ± 0.87	–2.5 ± 0.78	.696
Medications			
Metformin use (n, %)	0	15, 50	
Metformin + sulfonylurea use (n, %)	0	12, 40	
Metformin + sulfonylurea + insulin use (n, %)	0	3, 10	
Anti-osteoporotic treatment[a] (n, %)	2, 5	1, 3.3	

All data are expressed as mean ± SD

Abbreviations: na, not applicable; HbA1c, glycosylated hemoglobin A1c; ALP, alkaline phosphatase; FN, femoral neck; aBMD, areal bone mineral density.

[a]Bisphosphonate (alendronate).

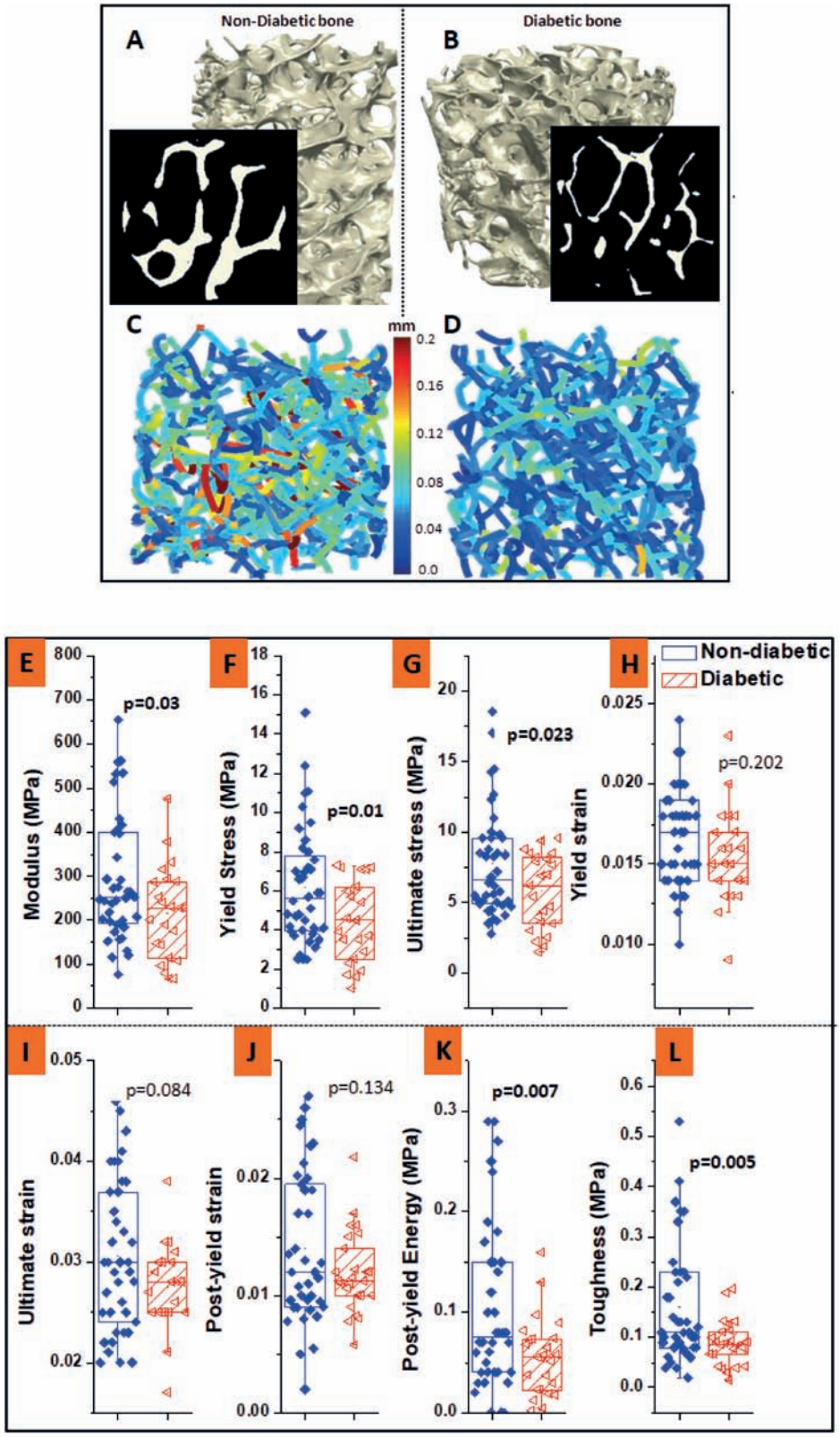

Figure 3. Representative 3D reconstructed μ-CT image. (A) represents the nondiabetic group and (B) represents the diabetic group. The color map in (C) and (D) represents the variation in trabecular thickness for nondiabetic and diabetic group respectively. (E-L) Elastic modulus, yield stress, ultimate stress, yield strain, ultimate strain, postyield strain, postyield energy, and toughness respectively, for the diabetic and nondiabetic groups.

Table 2. Findings on Structural and Compositional Determinants of Bone Quality

Characterization techniques		Parameters studied	Study groups		
			Nondiabetic	Diabetic	*P* value
Structural Parameter (Micro- CT)		Bone volume fraction (BV/TV) (%)	21.6 ± 5.50	18.53 ± 5.37	.031[a]
		Trabecular thickness (Tb.Th, mm)	0.167 ± 0.029	0.149 ± 0.026	.019[a]
		Trabecular separation (Tb.Sp, mm)	0.603 ± 0.149	0.677 ± 0.166	.095
		Trabecular number (Tb.N, 1/mm)	1.25 ± 0.176	1.15 ± 0.136	.033 [a]
		Structure model index (SMI)	1.92 ± 0.12	2.39 ± 0.19	.037[a]
		Degree of anisotropy (DA)	0.612 ± 0.102	0.579±0.198	.475
Composition (TGA)		Water (weight %)	14.8 ± 9.4	11.6 ± 6.2	.335
		Organic (weight %)	43.4 ± 9.5	50.8 ± 10.1	.087
		Mineral (dry weight %)	49.3 ± 7.5	40.9 ± 10.7	.038[a]
		Carbonate (weight %)	1.67 ± 0.3	1.67 ± 0.4	.988
Macro molecular vibrations (FTIR)	Protein structure	Amide I position (cm^{-1})	1643.8 ± 6.3	1647.3 ± 4.4	.02[a]
		Amide II position (cm^{-1})	1543.1 ± 6.1	1547.8 ± 7.02	.009[b]
	Protein content	Amide I band area/1450 band area	6.97 ± 3.87	3.67 ± 2.08	<.001[c]
		Amide II band area/1450 band area	2.56 ± 1.47	1.22 ± .91	<.001[c]

[a]$P < .05$, [b]$P < .01$, and [c]$P < .001$ respectively compared to nondiabetic group, data is expressed as mean ± SD

and the mean values of microstructural parameters are shown in Table 2. The diabetic group had significantly lower BV/TV (14.21%, $P = .03$), Tb.Th (mm) (10.8%, $P = .019$) and Tb.N (1/mm) (8.0%, $P = .033$), higher Tb.Sp (mm) (12.27%, $P = .095$) and SMI)(24.48%, $P = .037$) than the nondiabetic group. We observed similar mean values ($P = .475$) of DA among both groups. The mean value of SMI for the diabetic and nondiabetic groups is 2.39 ± 0.19 and 1.92 ± 0.12, respectively ($P = .037$), indicating that the rod-like trabeculae structure is dominant in the diabetic group compared with nondiabetics.

Mechanical Properties

The mean values of modulus, yield stress, ultimate stress, yield strain, ultimate strain, postyield strain, postyield energy, and toughness for both groups are shown in (Fig. 3 E-3L). The modulus, yield stress, ultimate stress, postyield energy, and toughness were found to be lower by 25% ($P = .03$), 27% ($P = .01$), 25% ($P = .02$), 47% ($P = .007$), and 45% ($P = .005$), respectively, in the diabetic group than in the nondiabetic group. These results indicate that the load-bearing and energy absorption capacity is significantly compromised in the diabetic bone. However, yield strain, ultimate strain, and postyield strain did not differ across groups.

Material Properties

Nanoindentation tests for both the groups reveal that under the same load of 3000 μN, the diabetic group had significantly lower values of modulus (7.37 ± 2.96 GPa to 9.0 ± 2.7 GPa, $P = .033$) and hardness (0.294 ± 0.150 GPa to 0.444 ± 0.152 GPa, $P = .014$) than the nondiabetic group. The modulus and hardness were found to be lower by 18.1% and 33.8%, respectively in the diabetic group as compared to the nondiabetic group (Fig. 4A and 4B).

Composition

Representative TGA curves of weight (%) vs temperature with their respective first derivatives are plotted in (Fig. 4C). The percentage of weight associated with water content (m24°C [%] to m200°C [%]), organic content (m200°C [%] to m600°C [%]), mineral content (m600°C [%]/m200°C [%]), and carbonate content (m600°C [%] to m800°C [%]) are shown in Table 2. Diabetic bones exhibited decreased mineral content ($P = .038$) compared with nondiabetics. No significant differences are found in the organic content ($P = .087$), water content ($P = .335$), and carbonate content ($P = .988$). Mineral/matrix ratio indicate that diabetic bones had lower mineral/matrix ratio compared with nondiabetics ($P = .016$) as shown in (Fig. 4D).

Mean Mineral Crystal Size

The representative XRD pattern of trabecular bone is shown in (Fig. 5A). The mean crystal length was not different between the groups (Fig. 5B), whereas diabetic bone had significantly larger crystal width than the nondiabetic bones (8.12 ± 2.07 nm vs 6.57 ± 1.33 nm, $P = .024$) as shown in (Fig. 5C).

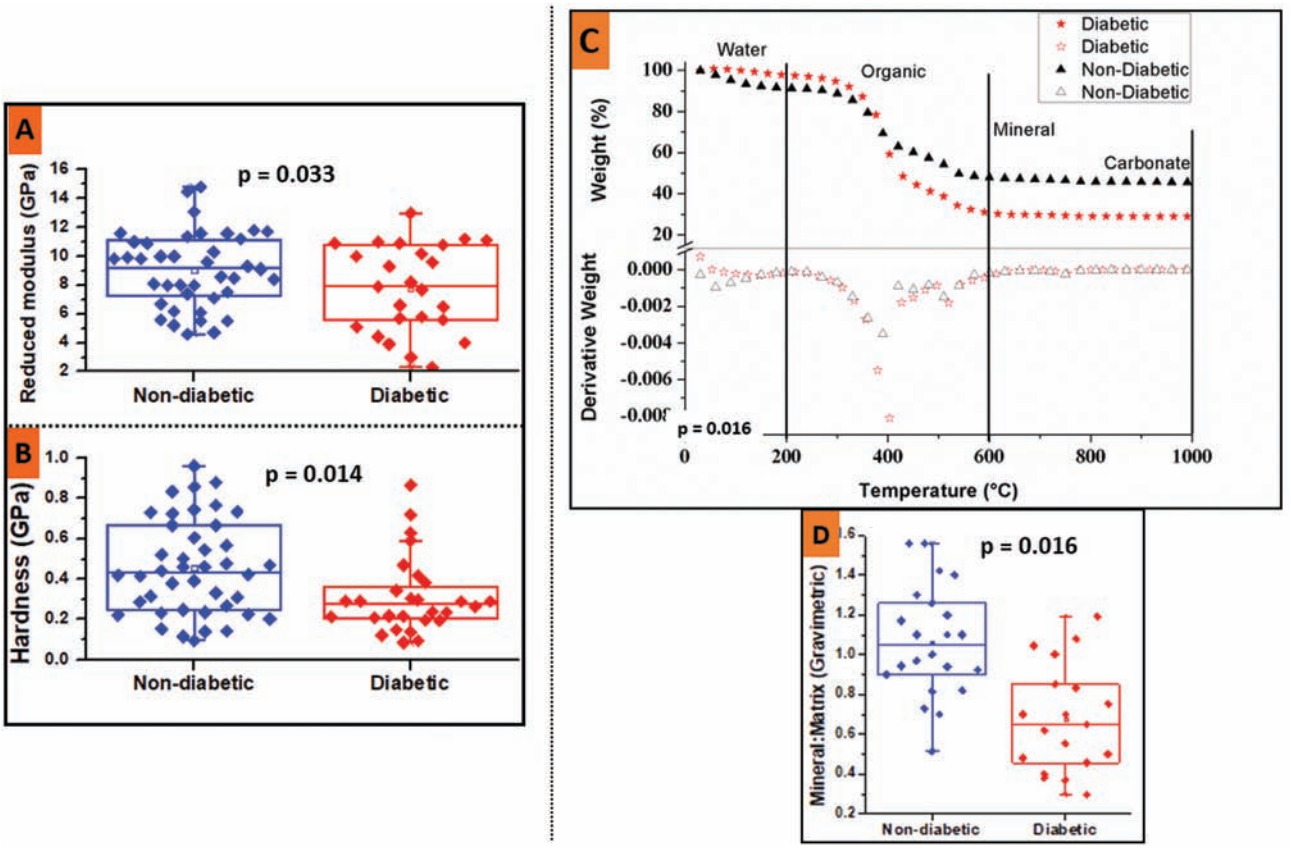

Figure 4. (A,B) Reduced modulus (Er) and hardness respectively obtained from nanoindentation, showing smaller value in the diabetic (T2D) group. (C) Representative TGA curves with their respective first derivatives for diabetic and nondiabetic femur trabecular bone heated to 1000°C. The TGA first derivative plots represent the more accurate temperature values associated with the percentage of mass lost, here it can be observed that superficial water completely evaporates before 200°C, and between 200 and 600°C the degradation and combustion of the bone matrix occurs. (D) Mineral to matrix ratio graph, showing a smaller ratio in the diabetic group $*P < .05$.

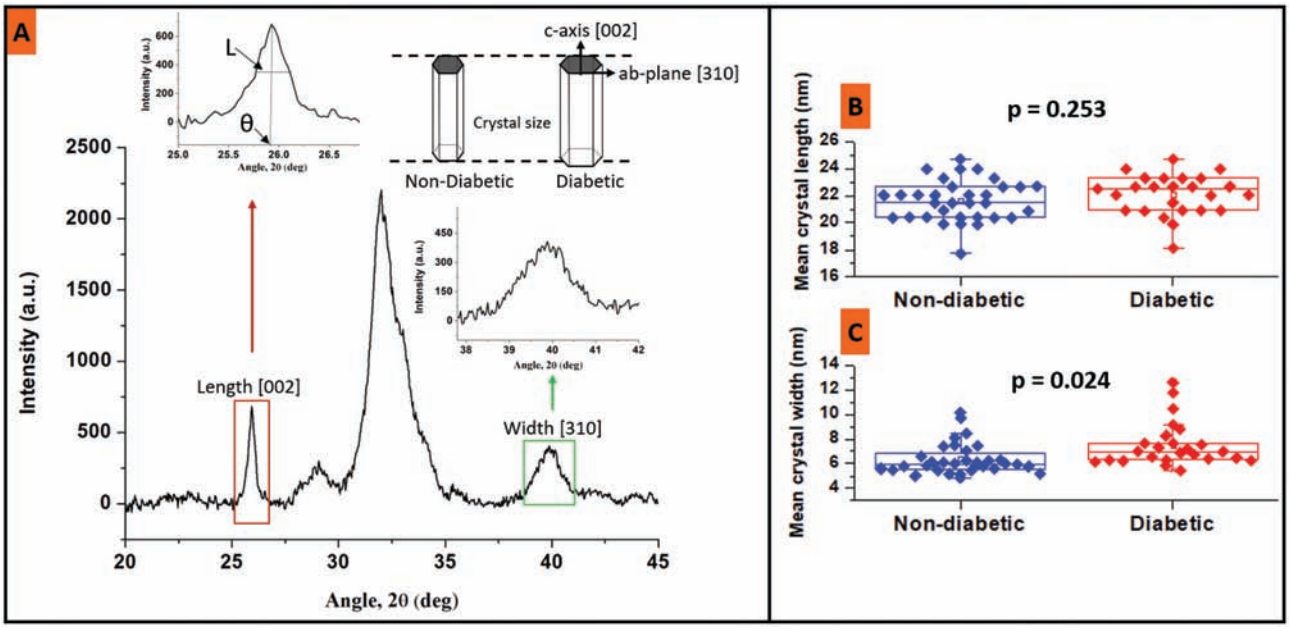

Figure 5. (A) Representative XRD pattern ($20° < 2\theta < 45°$) of human femoral trabecular bone. The peak at 26° and 40° is used to determine the average crystal length and width in the c-axis direction and ab-plane respectively according to Scherrer equation $B(2\theta) = \lambda/L\text{Cos}\theta$. Where, B is the mean crystal size, λ is the X-ray wavelength (1.5406 A°), L is the peak width at half maximum and θ is the Bragg angle where the peak is located. (B,C) Mean crystal size graph, showing the insignificant difference in average crystal length but wider width of mean crystal in the diabetic group

Mineral and Collagen Properties

The representative FTIR spectra of bone with the appropriate label of various bands and schematic presentation of enzymatic and nonenzymatic collagen crosslinks are shown in (Fig. 6A-6C). The mineral-based parameters including mineral crystallinity (P = .073), carbonate/phosphate ratio (P = .58), and acid phosphate content (P = .84) were not significantly different between the groups (Fig. 6 D-6F).

The collagen cross-links (NE-xLR [area ratio of 1678/1692 cm^{-1} sub-bands], E-xLR [area ratio of 1660/1678 cm^{-1} sub-bands]) and collagen maturity (area ratio of 1660/1690 cm^{-1}) are shown in (Fig. 6 G-6I). The diabetic bone had significantly higher NE-xLR (by 46.6%, P = .008) and lower E-xLR (by 35%, P = .032) than the nondiabetic bone, whereas no significant difference was observed in collagen maturity. Further, the diabetic bone had lower mineral/matrix ratio (by 21.1%, P = .046) as shown in (Fig. 6J).

Table 2 shows the shift in the position of Amide I (P = .02) and Amide II (P = .009) bands. The diabetic group had a lower value of area under the normalized peaks of Amide I and Amide II bands by 47.36% (P < .001) and 52.4% (P < .001), respectively, compared with the nondiabetic group. These results indicate that the secondary structure of Amide I and Amide II proteins is altered and the quantity of these proteins is lower in the diabetic bone.

Florescent Advanced Glycation End-products

The diabetic bone had 32.1% higher fAGE concentration than the nondiabetic bone (443 ± 198 vs 335 ± 155 ng quinine/mg collagen, P = .015) as reported in (Fig. 7A).

Interrelationships between Variables

Preoperative HbA1c was positively correlated with fAGEs (r = 0.635, P < .001) and NE-xLR (r = 0.561, P = .006). Correlations between HbA1c and mechanical properties revealed that within diabetic group HbA1c is significantly and negatively correlated with postyield energy (r = –0.402, P = .047), whereas this relationship was not significant in the nondiabetic group. Other than the reported parameters, none of the parameters were correlated with HbA1c. Furthermore, fAGEs were negatively correlated with mineral/matrix ratio (r = –0.487, P = .016), BV/TV (r = –0.488, P = .021), Tb.Th (r = –0.454, P = .044), and positively correlated with NE-xLR (r = 0.367, P = .045). The fAGEs were also negatively correlated with mechanical properties including postyield energy (r = –0.489, P = .013) and toughness (r = –0.441, P = .027) in the diabetic group as shown in (Fig. 7 B and 7C). Additionally, the NE-xLR was negatively correlated with the postyield strain (r = –0.433, P = .031) in diabetic but not in the nondiabetic group as shown in (Fig. 7D). The detailed correlation analysis of selected significant variables is reported in Table 3 and Table 4 for diabetic and nondiabetic groups, respectively.

ANCOVA comparing the effect of change in BV/TV on the change in mechanical properties between groups demonstrated that both regression slopes and intercept for modulus, yield stress, and ultimate stress were similar between groups as shown in (Fig. 8A-8C), respectively. The regression slopes of postyield energy (P = .792) and toughness (P = .977) were also similar between groups, whereas the intercept was significantly lower in diabetic group for these properties (P = .028) and (P = .032) (Fig. 8 D and 8E). These results reveal that the magnitude of change in BV/TV does not account for the differences in postyield properties observed between the 2 groups.

Forward stepwise regression tests to predict mechanical properties as a dependent variable using all significant parameters as independent variables showed that in the diabetic group the BV/TV, fAGEs, and mineral to matrix ratio (FTIR) can explain up to 86.7% (P < .001) of variance in ultimate strength, whereas in the nondiabetic group only BV/TV was observed to be a significant predictor explaining up to 39.8% of the variance in ultimate strength. Mineral to matrix ratio (FTIR) and Tb.Th were found to predict yield strain up to 77.4% (P < .001) in the diabetic group.

The power of study was performed by comparing the mean value of postyield energy and toughness between diabetic and nondiabetic groups, this outcome was found to be 88% and 82% respectively.

Discussion

This is the first investigation linking biomechanical, microstructural, material, and compositional properties of human bone in individuals with diabetes and known fragility fractures. Our findings provide evidence of detrimental effects of hyperglycemia on trabecular bone quality at multiple organizational scales leading to lower energy absorption and toughness, which can explain the increased bone fragility in patients with T2D.

The overall loss in bone quality and strength may be governed by a cascade of events happening at different length scales, such as abnormalities in the mineral and collagen quality at the nanoscale, accumulation of unrepaired microdamage or microcracks at the microscale, and changes in the trabecular architecture and a decrease in the trabecular connectivity at the mesoscale. Furthermore, any alteration in the properties locally, either at the micro- or

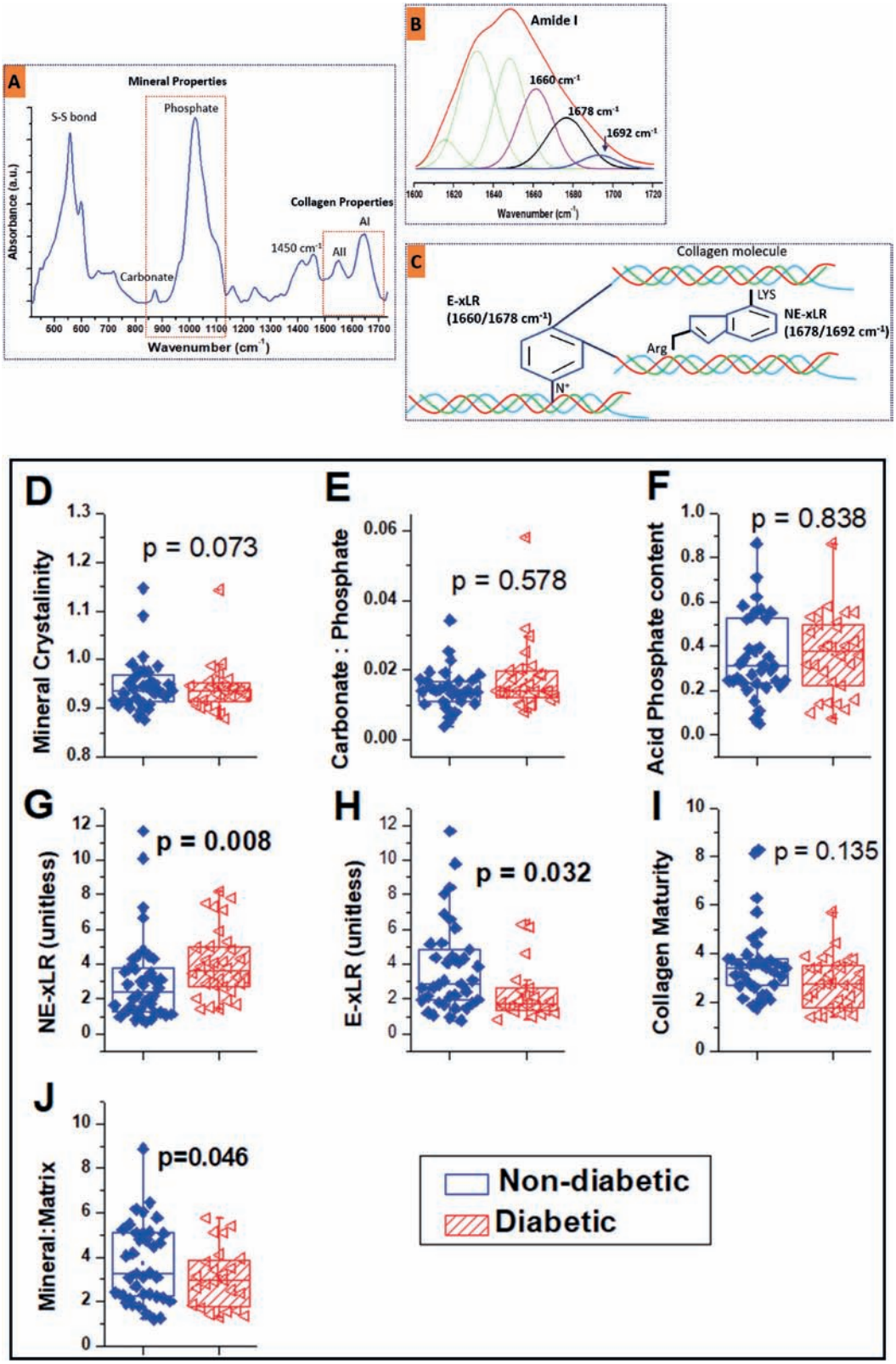

Figure 6. (A) Representative FTIR spectra with the appropriate label of various bands to analyze the diabetic and nondiabetic femoral trabecular bone. (B) Peak fitting of Amide I band, collagen properties were obtained by peak fitting of Amide I band with sub-bands (Gaussian curves) at 1610, 1630, 1645, 1660, 1678, and 1692 cm^{-1}. (C) Scheme of the enzymatic (E-xL) and nonenzymatic crosslink (NE-xL) formation in bone collagen. (D-F) Measures of mineral properties, showing all mineral parameters could not reach to the level of significance. (G) Nonenzymatic cross-link ratio (NE-xLR [the area ratio of the 1678/1692 cm^{-1} sub-bands within the Amide I peak, total cross-linking AGEs]). (H) Enzymatic crosslink ratio (E-xLR, the area ratio of the 1660/1678 cm^{-1} sub-bands within the Amide I peak). (I) Collagen maturity (area ratio of the 1660/1692 cm^{-1} sub-bands within the Amide I peak). (J) Lower mineral:matrix ratio in the diabetic group. Abbreviations: AI, Amide I; AII, Amide II; E-xLR, enzymatic cross-link ratio; NE-xLR, nonenzymatic cross-link ratio; AGE, advanced glycation end product.

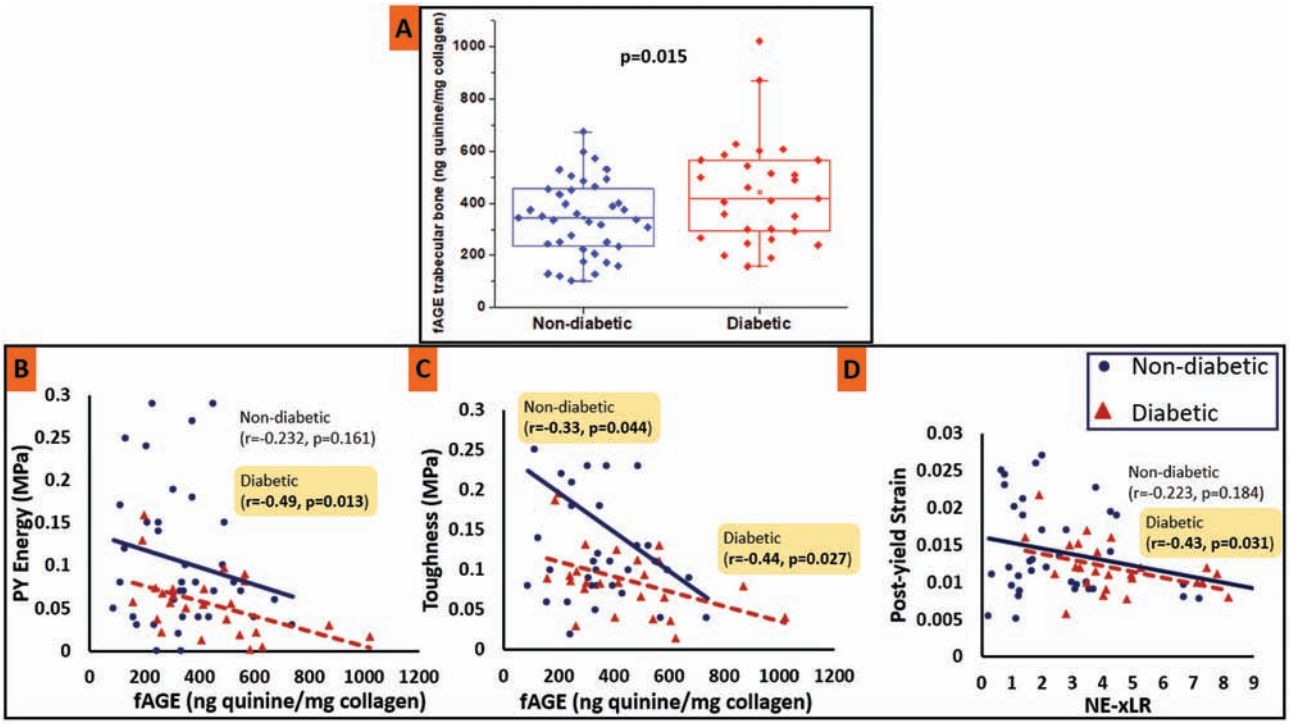

Figure 7. (A) Graph showing that the fAGE content is higher in the diabetic group. (B,C) Mechanical properties versus a measure of glycation (fAGE and NE-xLR). Graphical data for several mechanical parameters versus total fluorescent AGEs (B,C) and NE-xLR (D) are shown.

at the nanolevel, affects the properties of the hierarchical organization of bone at higher scales (53, 54). Thus, our findings of differences at nanoscale and microscale can be linked to each other and to higher scales to get a comprehensive diagnosis of altered bone quality and fracture risk in diabetes. To this end, forward stepwise regression analysis of multiscale data, presented here, shows that the BV/TV, fAGE, and mineral to matrix ratio (FTIR) can explain up to 86.7% of the variance in ultimate strength. Also, the mineral to matrix ratio (FTIR) and Tb.Th together can explain up to 77.4% of the variance in yield strain. Thus, in addition to bone microstructure (BV/TV, Tb.Th), nanoscale characteristics of bone (mineral to matrix ratio) and collagen quality (fAGEs) are important predictors of the loss in mechanical properties and the associated increase in fracture risk of diabetic bone.

The assessment of bone microstructure with μ-CT showed lower BV/TV (%) in diabetic patients than in nondiabetic patients. Moreover, the structure was noticeably altered, evidenced by the thinning of trabeculae and, in general, by fewer trabeculae. Indeed, due to this compromised bone microstructure, a lower value of ultimate stress (uniaxial compression) is observed in those with diabetes. The results of uniaxial compression tests found in our study are consistent with previously published studies (55-59). Our results of microstructural parameters are slightly different from those reported in earlier studies (10, 11, 13). However, in these studies bone tissue was obtained from individuals with obesity and/or severe arthritis, which could explain their findings of the same or increased BV/TV in those compared with diabetes. It is also possible that our study finding of lower BV/TV in diabetes is related to the distinct phenotypes of Asians (19, 60-64).

At the apparent level (uniaxial compression) and tissue level (nanoindentation), the lower value of modulus (stiffness), observed with the diabetic bone, are directly associated with decreased mineral to matrix ratio (FTIR). The wider crystal size without a change in length decreases the aspect ratio (surface area/volume) of apatite crystals and explains reduced elastic modulus of bone material (65). Furthermore, altered crystal shape also can affect crystal connectivity, orientation, and arrangement (65).

We also observed the increase in protein misfolding (altered secondary structure of proteins) and a decrease in relative protein content (Amide I and Amide II) in the diabetic bone. The altered secondary structure is primarily responsible for the change in the structural integrity of the collagen in bone (66). This altered collagen structure can change the hydration level of collagen, and/or change in shape, size, orientation, and growth of inorganic mineral content (67) as noted above.

One of the reasons for the degradation of bone quality in diabetes could be prolonged hyperglycemia (HbA1c), which may increase the accumulation of AGEs in the bone matrix. In correlation analysis, we found the HbA1c is positively correlated with fAGE content and NE-xLR. We

Table 3. Correlation analysis of selected significant variables of diabetic group which has at least 1 or more significant relationship with at least 1 other variable

Diabetic group	Modulus	Yield strength	Ultimate strength	Yield strain	Ultimate strain	Yield energy	PY energy	PY strain	Toughness	BVTV	HbA1c	fAGE	NE–xLR	E–xLR	M:M FTIR	Tb.Th
Modulus	1	0.710[a]	0.729[a]	–0.134	0.019	0.548[b]	0.485[b]	0.125	0.620[a]	0.674[a]	0.048	–0.122	0.187	0.376	0.158	0.41
Yield strength	0.710[a]	1	0.950[a]	0.306	0.247	0.924[a]	0.197	0.023	0.499[b]	0.655[a]	0.314	0.141	0.306	0.098	0.333	0.633[a]
Ultimate strength	0.729[a]	0.950[a]	1	0.239	0.299	0.842[a]	0.368	0.14	0.623[a]	0.749[a]	0.253	–0.292	0.294	0.133	0.37	0.670[a]
Yield strain	–0.134	0.306	0.239	1	0.558[a]	0.631[a]	–0.196	–0.172	0.085	0.117	0.111	0.031	0.017	–0.069	0.331	0.092
Ultimate strain	0.019	0.247	0.299	0.558[a]	1	0.395	0.144	0.722[a]	0.282	0.084	–0.119	0.025	–0.378	–0.082	0.233	0.155
Yield energy	0.548[b]	0.924[a]	0.842[a]	0.631[a]	0.395	1	0.154	–0.057	0.533[b]	0.560[a]	0.181	–0.032	0.207	0.032	0.459	0.493[b]
PY energy	0.485[b]	0.197	0.368	–0.196	0.144	0.154	1	0.306	0.919[a]	0.617[a]	–0.402[b]	–0.489[b]	0.042	0.156	0.273	0.484[b]
PY strain	0.125	0.023	0.14	–0.172	0.722[a]	–0.057	0.306	1	0.255	0.003	–0.238	0.028	–0.433[b]	–0.031	–0.033	0.108
Toughness	0.620[a]	0.499[b]	0.623[a]	0.085	0.282	0.533[b]	0.919[a]	0.255	1	0.747[a]	–0.331	–0.441[b]	0.094	0.157	0.38	0.613[a]
BV/TV	0.674[a]	0.655[a]	0.749[a]	0.117	0.084	0.560[a]	0.617[a]	0.003	0.747[a]	1	–0.159	–0.488[b]	0.051	0.526[b]	0.341	0.804[a]
HbA1c	0.048	0.314	0.253	0.111	–0.119	0.181	–0.402[b]	–0.238	–0.331	–0.159	1	0.635[a]	0.561[a]	–0.307	0.007	–0.269
fAGE	–0.122	0.141	–0.292	0.031	0.025	–0.032	–0.489[b]	0.028	–0.441[b]	–0.488[b]	0.635[a]	1	0.367[b]	–0.354	–0.487[b]	–0.454[b]
NE-xLR	0.187	0.306	0.294	0.017	–0.378	0.207	0.042	–0.433[b]	0.094	0.051	0.561[a]	0.367[b]	1	–0.37	0.112	–0.001
E-xLR	0.376	0.098	0.133	–0.069	–0.082	0.032	0.156	–0.031	0.157	0.526[b]	–0.307	–0.354	–0.37	1	–0.105	0.145
M:M FTIR	0.158	0.333	0.37	0.331	0.233	0.459	0.273	–0.033	0.38	0.341	0.007	–0.487[b]	0.112	–0.105	1	0.361
Tb.Th	0.41	0.633[a]	0.670[a]	0.092	0.155	0.493[b]	0.484[b]	0.108	0.613[a]	0.804[a]	–0.269	–0.454[b]	–0.001	0.145	0.361	1

Abbreviation: PY, postyield.

[a]Correlation is significant at the 0.01 level (2-tailed).

[b]Correlation is significant at the 0.05 level (2-tailed).

Table 4. Correlation analysis of selected significant variables of nondiabetic group which has at least 1 or more significant relationship with at least 1 other variable

Nondiabetic group	Modulus	Yield strength	Ultimate strength	Yield strain	Ultimate strain	Yield energy	PY energy	PY strain	Toughness	BVTV	HbA1c	fAGE	NE–xLR	E–xLR	M:M FTIR	Tb.Th
Modulus	1	0.791[a]	0.767[a]	0.122	0.164	0.292	0.545[a]	–0.058	0.477[a]	0.701[a]	–0.332[b]	–0.184	–0.028	0.253	0.261	0.341[b]
Yield strength	0.791[a]	1	0.974[a]	0.029	0.077	0.258	0.603[a]	–0.015	0.569[a]	0.746[a]	–0.274	–0.162	–0.033	0.076	0.197	0.441[a]
Ultimate strength	0.767[a]	0.974[a]	1	0.022	0.069	0.247	0.601[a]	–0.017	0.576[a]	0.698[a]	–0.291	–0.143	–0.035	0.069	0.224	0.431[a]
Yield strain	0.122	0.029	0.022	1	0.973[a]	0.972[a]	0.545[a]	–0.03	–0.02	0.029	0.039	–0.231	–0.094	0.405[b]	–0.035	–0.054
Ultimate strain	0.164	0.077	0.069	0.973[a]	1	0.958[a]	0.607[a]	0.087	0.079	0.078	–0.044	–0.283	–0.143	0.419[b]	–0.037	–0.039
Yield energy	0.292	0.258	0.247	0.972[a]	0.958[a]	1	0.675[a]	–0.042	0.124	0.192	–0.05	–0.272	–0.072	0.389[b]	0.008	0.067
PY energy	0.545[a]	0.603[a]	0.601[a]	0.545[a]	0.607[a]	0.675[a]	1	0.055	**0.815**[a]	**0.405**[b]	–0.243	–0.328[b]	–0.02	0.158	0.085	0.186
PY strain	–0.058	–0.015	–0.017	–0.03	0.087	–0.042	0.055	1	0.113	–0.121	0.105	–0.137	–0.223	0.097	–0.008	–0.1
Toughness	0.477[a]	0.569[a]	0.576[a]	–0.02	0.079	0.124	0.815[a]	0.113	1	**0.370**[b]	–0.283	–0.232	0.029	–0.147	0.102	0.211
BVTV	0.701[a]	0.746[a]	0.698[a]	0.029	0.078	0.192	0.405[b]	–0.121	0.370[b]	1	–0.266	0.009	–0.108	0.103	0.09	0.566[a]
HbA1c	–0.332[b]	–0.274	–0.291	0.039	–0.044	–0.05	–0.243	0.105	–0.283	–0.266	1	0.296[b]	0.396[a]	–0.353[b]	–0.057	–0.125
fAGE	–0.184	–0.162	–0.143	–0.231	–0.283	–0.272	–0.328[b]	–0.137	–0.232	0.009	0.296[b]	1	0.019	–0.111	–0.205	0.315[b]
NE-xLR	–0.028	–0.033	–0.035	–0.094	–0.143	–0.072	–0.02	–0.223	0.029	–0.108	0.396[a]	0.019	1	–0.430[a]	–0.107	–0.014
E-xLR	0.253	0.076	0.069	0.405[b]	0.419[b]	0.389[b]	0.158	0.097	–0.147	0.103	–0.353[b]	–0.111	–0.430[a]	1	0.128	0.219
M:M FTIR	0.261	0.197	0.224	–0.035	–0.037	0.008	0.085	–0.008	0.102	0.09	–0.057	–0.205	–0.107	0.128	1	–0.185
Tb.Th	0.341[b]	0.441[a]	0.431[a]	–0.054	–0.039	0.067	0.186	–0.1	0.211	0.566[a]	–0.125	0.315[b]	–0.014	0.219	–0.185	1

PY, post-yield

[a]Correlation is significant at the 0.01 level (2-tailed).

[b]Correlation is significant at the 0.05 level (2-tailed).

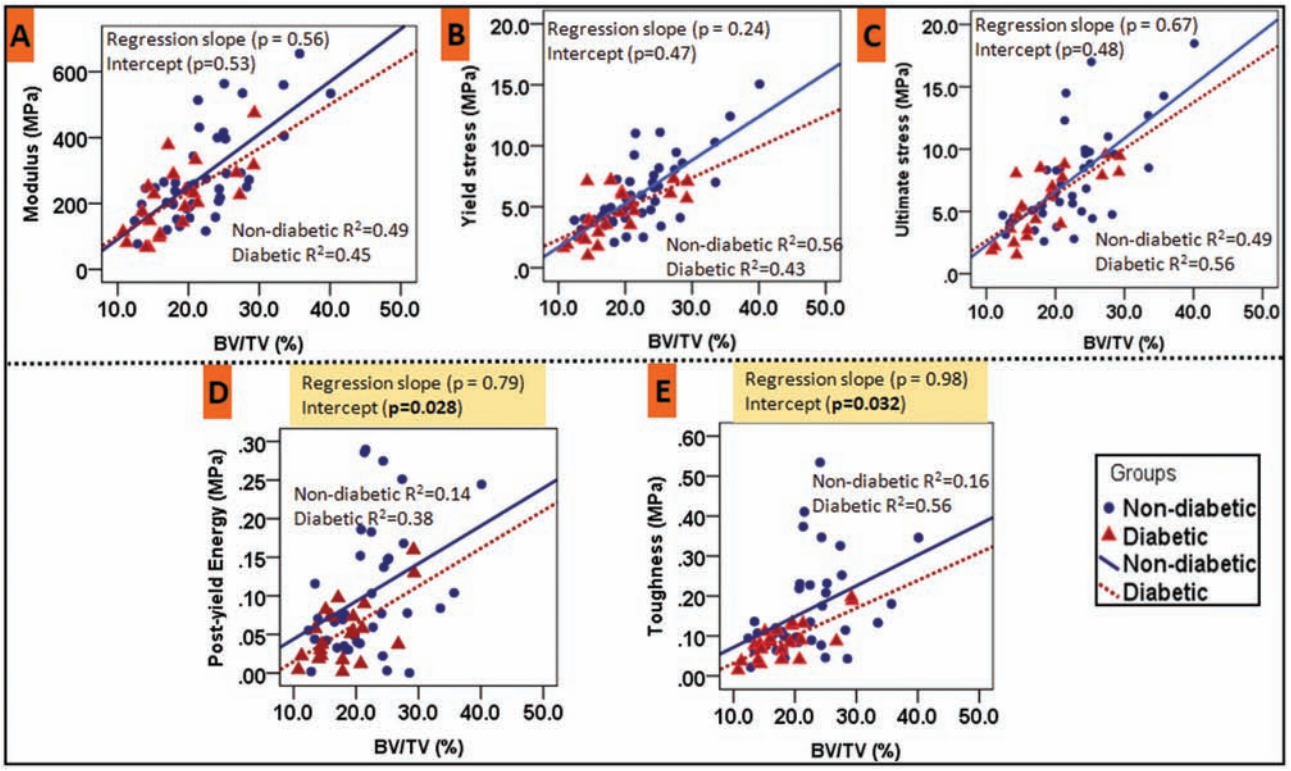

Figure 8. The relationships between bone volume fraction and (A) modulus, (B) yield stress, (C) ultimate stress, (D) postyield energy and (E) toughness between diabetic and nondiabetics are shown. Data are presented along with best-fit lines (solid lines).

also observed the reduced E-xLR and increased NE-xLR in the diabetic group compared with the nondiabetic group. The enzymatic crosslinks (E-xL, beneficial cross-links) are responsible for mechanical strength whereas NE-xL is associated with bone fragility (68-70). Our findings of reduced E-xLR and increased NE-xLR are evidence of AGE accumulation (NE-xL) in the bone, which induces tissue damage through structural modification of proteins and abnormal collagen fibril organization in the diabetic bone. The reduction of E-xLR can be associated with hyperglycemia and oxidative stress (OS) (71, 72). Further, the NE-xL (AGE accumulation) in diabetic bone favors material rigidity by restricting the uncoiling of the triple helical structure of collagen (flexibility) and confining the natural energy dissipation process during loading to a limited region (73). Such changes will alter the nature of microdamage formation in bone from diffuse cracking, characteristic of ductile materials, to linear microcracks, making bone more susceptible to the fracture (69, 74, 75). Indeed, in the present study, elevated levels of HbA1c, fAGEs, and NE-xLR correlated negatively with bone biomechanical properties—postyield energy, toughness, and postyield strain in diabetes. Also, the lower value of intercept of postyield energy and toughness in diabetic group (ANCOVA) revealed that the glycated bone exhibited lesser energy dissipation and reduced toughness. Our results are consistent with previously published studies that reported the accumulation of AGEs as a cause for abnormal collagen synthesis and altered collagen structure (76) in the bone. Thus, changes in collagen, mineral, altered bone composition at the nanoscale, and lower bone volume fraction and trabecular architecture at the microscale in diabetic group provides detailed insight on skeletal fragility in diabetes and improves the current understanding on the impact of diabetes on bone homeostasis.

In the present study, FN BMD T-scores were similar among those with T2D and without diabetes. The deficits in bone quality in T2D mentioned above underlie the compromised bone strength in diabetes. These findings explain the inability of BMD T-score, a quantitative measure, to accurately predict fracture risk in T2D as previously reported in large studies (4, 77). In the Study of Osteoporotic Fractures (4), for a given age and T-score, the risk of hip or nonspine fracture was higher in women with T2D than those without diabetes after 25 years of follow up. While the T-score is useful in fracture risk assessment in women with and without diabetes, the T-score underestimates fracture risk in T2D (4, 9).

Various techniques (pQCT, HRpQCT, Osteoprobe) have been used in research to investigate bone quality and bone strength. However, each technique presents its own challenges for utilization in routine clinical practice. In MrOS (77), pQCT was used to assess bone strength at peripheral

sites in T2D and lower bone bending strength was observed at mid shaft regions of radius and tibia in those with T2D, despite no differences in cortical vBMD. Though pQCT is a clinically available tool, the imaging resolution remains a limitation. Consequently, various approaches have been proposed to include changes in bone quality and explain poor bone mechanical properties, such as those reported here. For example, bone strength estimated by microfinite element analysis (micro-FEA/HR-pQCT) at the distal radius has been shown to be lower in T2D compared to controls (78). Similarly, micro-indentation of the tibial cortex has been performed to demonstrate that the estimated bone material strength index (BMSi) is decreased in T2D compared with controls (79-81). While these techniques have increased our understanding of bone fragility in diabetes, further work is needed to assess their application for routine clinical use. The only tool currently approved for clinical assessment of bone quality is trabecular bone score (5, 82), which helps to predict fracture risk, independent of BMD. However, trabecular bone score is a surrogate measurement of trabecular architecture and not a tool for assessment of bone strength. Hence, diagnostic tools are needed for specific and direct assessment of bone quality to aid clinical assessment of fracture risk in diabetes. Meanwhile, the International Osteoporosis Foundation recommends adjusting BMD T-score for diabetes to avoid underestimation of risk in clinical practice (9).

This study has some limitations. First, this study is limited to *ex vivo* assessments of bone quality in patients who underwent hip fragility fractures. Nonfracture controls with and without diabetes were not studied; however, it is not feasible to obtain femoral head specimen from healthy controls. Second, the study focuses exclusively on trabecular bone and does not include properties of cortical bone. Other studies have reported the increased cortical porosity (6, 12, 78) and altered cortical bone material properties in vivo, by demonstrating decreased BMSi (measured through Osteoprobe) in those with diabetes compared with controls (79, 80, 81). Also, the study lacks information on the effect of type of diabetes treatment (insulin, metformin, and other antidiabetic treatment) on bone properties. Sample sizes within each subgroup are small, and a large randomized clinical trial would be necessary to draw any meaningful conclusion regarding the effect of diabetes treatment on bone properties. Further, we could not assess bone remodeling via dynamic bone labeling. Lastly, we used femoral head specimens instead of femoral neck (typical fracture site) because in most cases of fracture, femoral necks are extensively and variably damaged either due to fracture or during surgery. Thus, it was difficult to obtain uniform specimens from all patients. Hence to avoid site-specific differences, we took samples from the femoral head.

Despite the above-mentioned limitations, our study's major strength is that the explants characterized here are from the patients with diabetes with known fragility fractures. Further, this study includes a wide range of duration and severity of the disease and this is an important and unique aspect of our study because longer duration of diabetes is typically required for skeletal changes in diabetes to fully manifest. The severity and duration of diabetes are known to greatly affect fracture risk (6, 83) and therefore it may also affect the degree of compositional changes. This aspect could also explain the differences between fAGEs results in our study and those reported in other studies (10, 11) where a significant difference in fAGEs was not observed between groups. One study (10) included samples for a shorter duration of disease of nearly two years, whereas in other study (11), the information on duration of diabetes was not reported. The results of our fAGEs content are consistent with 1 recent study (13) that found a 1.5-fold increase in fAGEs content in women with T2D of mean duration of nearly 15 years compared with nondiabetic women.

In conclusion, the study findings provide evidence that diabetes affects the trabecular bone quality at multiple organization levels. The accumulation of AGEs is 1 of the processes that favor deterioration of bone quality in diabetes leading to material, structural, compositional, and biomechanical dysfunctionality. Overall, together with altered structure and material properties, these novel findings of changes in the composition of bone explain the compromised mechanical performance and diminished bone strength in diabetes. Finally, this study demonstrates that whilst osteoporotic bones are fracture prone, diabetes is detrimental to bone quality, thus highlighting the need for more specific measures to understand and diagnose bone quality and bone fragility in T2D.

Acknowledgments

The IIT Ropar and PGIMER Chandigarh are acknowledged for providing the infrastructure and facilities used in the current research. The authors acknowledge Mr. Aakash Soni for his help in editing the manuscript for grammar and proofreading. The authors acknowledge Dr. Atharva Poundarik for his help in statistical analysis at multiscale and intellectual discussion during the preparation of manuscript.

Financial Support: The Department of Science and Technology, India (CRG/2018/002219) and IMPRINT - Ministry of Human Resource Development, India (IMP/2019/000150) are acknowledged for providing the necessary funds.

Author Contributions: P.S. designed the experiments, conducted experiments, analyzed and interpreted the data, and wrote the manuscript, R.N.Y. designed the micro-CT and Uniaxial compression experiments, performed experiments, and analyzed the data, V.D., J.C.B., D.N., S.K. were involved in all data collection, S.S., S.A., V.G.G., did data collection, data interpretation and revising the manuscript con-

tent, V.M. revised the manuscript content, D.V. provided input on multiscale analysis of data, interpretation of results and edited the manuscript; R.D. provided clinical expertise, input on interpretation of results, and edited the manuscript; S.K.B, and N.K. identified the research problem and supervised the entire work at every step.

Additional Information

Correspondence: Sanjay Kumar Bhadada, Department of Endocrinology, PGIMER, India, Chandigarh, 160012, India. Email: bhadadask@rediffmail.com; or Navin Kumar, Department of Mechanical Engineering, Indian Institute of Technology Ropar, Rupnagar, Punjab, 140001, India. Email: nkumar@iitrpr.ac.in.

Disclosures: The authors have nothing to disclose.

Data Availability: The datasets generated during and/or analyzed during the current study are available from the corresponding authors on reasonable request.

References

1. Palermo A, D'Onofrio L, Eastell R, Schwartz AV, Pozzilli P, Napoli N. Oral anti-diabetic drugs and fracture risk, cut to the bone: safe or dangerous? A narrative review. *Osteoporos Int*. 2015;**26**(8):2073-2089.
2. Karim L, Rezaee T, Vaidya R. The effect of type 2 diabetes on bone biomechanics. *Curr Osteoporos Rep*. 2019;**17**(5):291-300.
3. Janghorbani M, Van Dam RM, Willett WC, Hu FB. Systematic review of type 1 and type 2 diabetes mellitus and risk of fracture. *Am J Epidemiol*. 2007;**166**(5):495-505.
4. Schwartz AV, Vittinghoff E, Bauer DC, et al.; Study of Osteoporotic Fractures (SOF) Research Group; Osteoporotic Fractures in Men (MrOS) Research Group; Health, Aging, and Body Composition (Health ABC) Research Group. Association of BMD and FRAX score with risk of fracture in older adults with type 2 diabetes. *JAMA*. 2011;**305**(21):2184-2192.
5. Dhaliwal R, Cibula D, Ghosh C, Weinstock RS, Moses AM. Bone quality assessment in type 2 diabetes mellitus. *Osteoporos Int*. 2014;**25**(7):1969-1973.
6. Patsch JM, Burghardt AJ, Yap SP, et al. Increased cortical porosity in type 2 diabetic postmenopausal women with fragility fractures. *J Bone Miner Res*. 2013;**28**(2):313-324.
7. Starup-Linde J, Hygum K, Langdahl BL. Skeletal fragility in type 2 diabetes mellitus. *Endocrinol Metab (Seoul)*. 2018;**33**(3):339-351.
8. Farr JN, Khosla S. Determinants of bone strength and quality in diabetes mellitus in humans. *Bone*. 2016;**82**:28-34.
9. Ferrari SL, Abrahamsen B, Napoli N, et al.; Bone and Diabetes Working Group of IOF. Diagnosis and management of bone fragility in diabetes: an emerging challenge. *Osteoporos Int*. 2018;**29**(12):2585-2596.
10. Karim L, Moulton J, Van Vliet M, et al. Bone microarchitecture, biomechanical properties, and advanced glycation end-products in the proximal femur of adults with type 2 diabetes. *Bone*. 2018;**114**:32-39.
11. Hunt HB, Torres AM, Palomino PM, et al. Altered tissue composition, microarchitecture, and mechanical performance in cancellous bone from men with type 2 diabetes mellitus. *J Bone Miner Res*. 2019;**34**(7):1191-1206.
12. Wölfel EM, Jähn-Rickert K, Schmidt FN, et al. Individuals with type 2 diabetes mellitus show dimorphic and heterogeneous patterns of loss in femoral bone quality. *Bone*. 2020;140:115556.
13. Piccoli A, Cannata F, Strollo R, et al. Sclerostin regulation, microarchitecture, and advanced glycation end-products in the bone of elderly women with type 2 diabetes. *J Bone Miner Res*. 2020;35(12):2415-2422.
14. Gallant MA, Brown DM, Organ JM, Allen MR, Burr DB. Reference-point indentation correlates with bone toughness assessed using whole-bone traditional mechanical testing. *Bone*. 2013;**53**(1):301-305.
15. Rubin MR, Paschalis EP, Poundarik A, et al. Advanced glycation endproducts and bone material properties in type 1 diabetic mice. *PLoS One*. 2016;**11**(5):e0154700.
16. Marin C, Papantonakis G, Sels K, et al. Unraveling the compromised biomechanical performance of type 2 diabetes- and Roux-en-Y gastric bypass bone by linking mechanical-structural and physico-chemical properties. *Sci Rep*. 2018;**8**(1):5881.
17. Acevedo C, Sylvia M, Schaible E, et al. Contributions of material properties and structure to increased bone fragility for a given bone mass in the UCD-T2DM rat model of type 2 diabetes. *J Bone Miner Res*. 2018;**33**(6):1066-1075.
18. Hunt HB, Pearl JC, Diaz DR, King KB, Donnelly E. Bone tissue collagen maturity and mineral content increase with sustained hyperglycemia in the KK-Ay murine model of type 2 diabetes. *J Bone Miner Res*. 2018;**33**(5):921-929.
19. Sihota P, Yadav RN, Poleboina S, et al. Development of HFD-Fed/low-dose STZ-treated female Sprague-Dawley rat model to investigate diabetic bone fragility at different organization levels. *JBMR Plus*. 2020;**4**(10):e10379.
20. Thomas CJ, Cleland TP, Sroga GE, Vashishth D. Accumulation of carboxymethyl-lysine (CML) in human cortical bone. *Bone*. 2018;**110**:128-133.
21. Gkogkolou P, Bohm M, Böhm M. Advanced glycation end products: key players in skin ageing? *Gkogkolou, Paraskevi Bohm, Markus*. 2012;**4**(3):259-270.
22. Schmidt FN, Zimmermann EA, Campbell GM, et al. Assessment of collagen quality associated with non-enzymatic cross-links in human bone using Fourier-transform infrared imaging. *Bone*. 2017;**97**:243-251.
23. Burr DB. Changes in bone matrix properties with aging. *Bone*. 2019;**120**:85-93.
24. American Diabetes Association (ADA). Standard of medical care in diabetes - 2017. *Diabetes Care*. 2017;**40**(suppl 1):s4-s128.
25. Doube M, Kłosowski MM, Arganda-Carreras I, et al. BoneJ: free and extensible bone image analysis in ImageJ. *Bone*. 2010;**47**(6):1076-1079.
26. Bouxsein ML, Boyd SK, Christiansen BA, Guldberg RE, Jepsen KJ, Müller R. Guidelines for assessment of bone microstructure in rodents using micro-computed tomography. *J Bone Miner Res*. 2010;**25**(7):1468-1486.
27. Wang J, Zhou B, Liu XS, et al. Trabecular plates and rods determine elastic modulus and yield strength of human trabecular bone. *Bone*. 2015;**72**:71-80.
28. Zdero R. *Experimental Methods in Orthopaedic Biomechanics*. Elsevier Inc.; 2017.
29. An YH, Draughn RA. Mechanical testing of bone and the bone implant interface. CRC Press; 1999:648.

30. Karim L, Vashishth D. Heterogeneous glycation of cancellous bone and its association with bone quality and fragility. *PLoS One*. 2012;**7**(4):e35047.
31. Bhushan B. Depth-sensing nanoindentation measurement techniques and applications. *Microsyst Technol*. 2017;**23**(5):1595-1649.
32. Saini K, Discher D, Kumar N. Static and time-dependent mechanical response of organic matrix of bone. *J Mech Behav Biomed Mater*. 2019;**91**:315-325.
33. Edward Hoffler C, Edward Guo X, Zysset PK, Goldstein SA. An application of nanoindentation technique to measure bone tissue lamellae properties. *J Biomech Eng*. 2005;**127**(7):1046-1053.
34. Rodriguez-Florez N, Oyen ML, Shefelbine SJ. Insight into differences in nanoindentation properties of bone. *J Mech Behav Biomed Mater*. 2013;**18**:90-99.
35. Oliver WC, Pharr GM. An improved technique for determining hardness and elastic modulus using load and displacement sensing indentation experiments. *J Mater Res*. 1992;**7**(06):1564-1583.
36. Das R, Kumar A, Patel A, Vijay S, Saurabh S, Kumar N. Biomechanical characterization of spider webs. *J Mech Behav Biomed Mater*. 2017;**67**:101-109.
37. Rodriguez-Florez N, Garcia-Tunon E, Mukadam Q, et al. An investigation of the mineral in ductile and brittle cortical mouse bone. *J Bone Miner Res*. 2015;**30**(5):786-795.
38. Mkukuma LD, Imrie CT, Skakle JM, Hukins DW, Aspden RM. Thermal stability and structure of cancellous bone mineral from the femoral head of patients with osteoarthritis or osteoporosis. *Ann Rheum Dis*. 2005;**64**(2):222-225.
39. Farlay D, Panczer G, Rey C, Delmas PD, Boivin G. Mineral maturity and crystallinity index are distinct characteristics of bone mineral. *J Bone Miner Metab*. 2010;**28**(4):433-445.
40. Turunen MJ, Kaspersen JD, Olsson U, et al. Bone mineral crystal size and organization vary across mature rat bone cortex. *J Struct Biol*. 2016;**195**(3):337-344.
41. Vetter U, Eanes ED, Kopp JB, Termine JD, Robey PG. Changes in apatite crystal size in bones of patients with osteogenesis imperfecta. *Calcif Tissue Int*. 1991;**49**(4):248-250.
42. Boskey A, Mendelsohn R. Infrared analysis of bone in health and disease. *J Biomed Opt*. 2005;**10**(3):031102.
43. Spevak L, Flach CR, Hunter T, Mendelsohn R, Boskey AL. FTIRI parameters describing acid phosphate substitution in biologic hydroxyapatite. *Calcif Tissue Int*. 2013;**92**(5):418-428.
44. Paschalis EP, Gamsjaeger S, Tatakis DN, Hassler N, Robins SP, Klaushofer K. Fourier transform Infrared spectroscopic characterization of mineralizing type I collagen enzymatic trivalent cross-links. *Calcif Tissue Int*. 2015;**96**(1):18-29.
45. Farlay D, Duclos ME, Gineyts E, et al. The ratio 1660/1690 cm(-1) measured by infrared microspectroscopy is not specific of enzymatic collagen cross-links in bone tissue. *PLoS One*. 2011;**6**(12):e28736.
46. Bozkurt O, Severcan M, Severcan F. Diabetes induces compositional, structural and functional alterations on rat skeletal soleus muscle revealed by FTIR spectroscopy: a comparative study with EDL muscle. *Analyst*. 2010;**135**(12):3110-3119.
47. Gu C, Katti DR, Katti KS. Microstructural and photoacoustic infrared spectroscopic studies of human cortical bone with osteogenesis imperfecta. *JOM*. 2016;**68**(4):1116-1127.
48. Sihota P, Yadav RN, Dhiman V, Bhadada SK, Mehandia V, Kumar N. Investigation of diabetic patient's fingernail quality to monitor type 2 diabetes induced tissue damage. *Sci Rep*. 2019;**9**(1):3193.
49. Towler MR, Wren A, Rushe N, Saunders J, Cummins NM, Jakeman PM. Raman spectroscopy of the human nail: a potential tool for evaluating bone health? *J Mater Sci Mater Med*. 2007;**18**(5):759-763.
50. Poundarik AA, Wu PC, Evis Z, et al. A direct role of collagen glycation in bone fracture. *J Mech Behav Biomed Mater*. 2015;**52**:120-130.
51. Sroga GE, Siddula A, Vashishth D. Glycation of human cortical and cancellous bone captures differences in the formation of Maillard reaction products between glucose and ribose. *PLoS One*. 2015;**10**(2):e0117240.
52. Eastoe JE. The amino acid composition of mammalian collagen and gelatin. *Biochem J*. 1955;**61**(4):589-600.
53. Rai RK, Sinha N. Dehydration-induced structural changes in the collagen-hydroxyapatite interface in bone by high-resolution solid-state NMR spectroscopy. *J Phys Chem C*. 2011;**115**(29):14219-14227.
54. Sabet FA, Raeisi Najafi A, Hamed E, Jasiuk I. Modelling of bone fracture and strength at different length scales: a review. *Interface Focus*. 2016;**6**(1):20150055.
55. Lv H, Zhang L, Yang F, et al. Comparison of microstructural and mechanical properties of trabeculae in femoral head from osteoporosis patients with and without cartilage lesions: a case-control study Pathophysiology of musculoskeletal disorders. *BMC Musculoskelet Disord*. 2015;**16**(1):1-10.
56. Aleixo I, Vale AC, Lúcio M, et al. A method for the evaluation of femoral head trabecular bone compressive properties. *Mater Sci Forum*. 2013;**730–732**(January):3-8.
57. Wolfram U, Wilke HJ, Zysset PK. Damage accumulation in vertebral trabecular bone depends on loading mode and direction. *J Biomech*. 2011;**44**(6):1164-1169.
58. Giulia M, Alessio D, Gabriela C, et al. Osteoporosis-related variations of trabecular bone properties of proximal human humeral heads at different scale lengths. *J Mech Behav Biomed Mater*. 2019;**100**(April):103373.
59. Hambli R. Micro-CT finite element model and experimental validation of trabecular bone damage and fracture. *Bone*. 2013;**56**(2):363-374.
60. Walsh JS, Vilaca T. Obesity, Type 2 Diabetes and Bone in Adults. *Calcif Tissue Int*. 2017;**100**(5):528-535.
61. Cho YM. Characteristics of the pathophysiology of type 2 diabetes in Asians. *Ann Laparosc Endosc Surg*. 2017;**2**:14.
62. Chan JC, Yeung R, Luk A. The Asian diabetes phenotypes: challenges and opportunities. *Diabetes Res Clin Pract*. 2014;**105**(1):135-139.
63. Fukushima M, Usami M, Ikeda M, et al. Insulin secretion and insulin sensitivity at different stages of glucose tolerance: a cross-sectional study of Japanese type 2 diabetes. *Metabolism*. 2004;**53**(7):831-835.
64. Matsumoto K, Miyake S, Yano M, et al. Glucose tolerance, insulin secretion, and insulin sensitivity in nonobese and obese Japanese subjects. *Diabetes Care*. 1997;**20**(10):1562-1568.
65. Vanleene M, Porter A, Guillot P-V, Boyde A, Oyen M, Shefelbine S. Ultra-structural defects cause low bone matrix stiffness despite high mineralization in osteogenesis imperfecta mice. *Bone*. 2012;**50**(6):1317-1323.

66. Napoli N, Chandran M, Pierroz DD, Abrahamsen B, Schwartz AV, Ferrari SL; IOF Bone and Diabetes Working Group. Mechanisms of diabetes mellitus-induced bone fragility. *Nat Rev Endocrinol*. 2017;**13**(4):208-219.
67. Rai RK, Singh C, Sinha N. Predominant role of water in native collagen assembly inside the bone matrix. *J Phys Chem B*. 2015;**119**(1):201-211.
68. Saito M, Kida Y, Kato S, Marumo K. Diabetes, collagen, and bone quality. *Curr Osteoporos Rep*. 2014;**12**(2):181-188.
69. Saito M, Marumo K. Collagen cross-links as a determinant of bone quality: a possible explanation for bone fragility in aging, osteoporosis, and diabetes mellitus. *Osteoporos Int*. 2010;**21**(2):195-214.
70. Viguet-Carrin S, Garnero P, Delmas PD. The role of collagen in bone strength. *Osteoporos Int*. 2006;**17**(3):319-336.
71. Fu M-X, Requena JR, Jenkins AJ, Lyons TJ, Baynes JW, Thorpe SR. The advanced glycation end product, N -(Carboxymethyl)lysine, is a product of both lipid peroxidation and glycoxidation reactions. *J Biol Chem*. 2002;**271**(17):9982-9986.
72. Saito M, Marumo K. Bone quality in diabetes. *Front Endocrinol (Lausanne)*. 2013;**4**:72.
73. Nair AK, Gautieri A, Chang SW, Buehler MJ. Molecular mechanics of mineralized collagen fibrils in bone. *Nat Commun*. 2013;**4**:1724.
74. Vashishth D, Gibson GJ, Khoury JI, Schaffler MB, Kimura J, Fyhrie DP. Influence of nonenzymatic glycation on biomechanical properties of cortical bone. *Bone*. 2001;**28**(2):195-201.
75. Tang SY, Vashishth D. The relative contributions of nonenzymatic glycation and cortical porosity on the fracture toughness of aging bone. *J Biomech*. 2011;**44**(2):330-336.
76. Wongdee K, Charoenphandhu N. Update on type 2 diabetes-related osteoporosis. *World J Diabetes*. 2015;**6**(5):673-678.
77. Petit MA, Paudel ML, Taylor BC, et al.; Osteoporotic Fractures in Men (MrOs) Study Group. Bone mass and strength in older men with type 2 diabetes: the Osteoporotic Fractures in Men Study. *J Bone Miner Res*. 2010;**25**(2):285-291.
78. Burghardt AJ, Issever AS, Schwartz AV, et al. High-resolution peripheral quantitative computed tomographic imaging of cortical and trabecular bone microarchitecture in patients with type 2 diabetes mellitus. *J Clin Endocrinol Metab*. 2010;**95**(11):5045-5055.
79. Nilsson AG, Sundh D, Johansson L, et al. Type 2 diabetes mellitus is associated with better bone microarchitecture but lower bone material strength and poorer physical function in elderly women: a population-based study. *J Bone Miner Res*. 2017;**32**(5):1062-1071.
80. Furst JR, Bandeira LC, Fan WW, et al. Advanced glycation endproducts and bone material strength in type 2 diabetes. *J Clin Endocrinol Metab*. 2016;**101**(6):2502-2510.
81. Farr JN, Drake MT, Amin S, Melton LJ 3rd, McCready LK, Khosla S. In vivo assessment of bone quality in postmenopausal women with type 2 diabetes. *J Bone Miner Res*. 2014;**29**(4):787-795.
82. Leslie WD, Aubry-Rozier B, Lamy O, Hans D; Manitoba Bone Density Program. TBS (trabecular bone score) and diabetes-related fracture risk. *J Clin Endocrinol Metab*. 2013;**98**(2):602-609.
83. Leanza G, Maddaloni E, Pitocco D, et al. Risk factors for fragility fractures in type 1 diabetes. *Bone*. 2019;**125**:194-199.